TISSUE ENGINEERING: Part A
Volume 23, Numbers 17 and 18, 2017

DOI: 10.1089/ten.tea.2016.0470

termis
Tissue Engineering
& Regenerative Medicine
International Society

SPECIAL FOCUS: STRATEGIC DIRECTIONS IN MUSCULOSKELETAL TISSUE ENGINEERING*

Meltblown Polymer Fabrics as Candidate Scaffolds for Rotator Cuff Tendon Tissue Engineering

Thomas L. Jenkins, BSE,[1,2] Sean Meehan, MS,[2] Behnam Pourdeyhimi, PhD,[3] and Dianne Little, DVM, PhD[1,2]

Various biomaterial technologies are promising for tissue engineering, including electrospinning, but commercial scale-up of throughput is difficult. The goal of the study was to evaluate meltblown fabrics as candidate scaffolds for rotator cuff tendon tissue engineering. Meltblown poly(lactic acid) fabrics were produced with several polymer crystallinities and airflow velocities [500(low), 900(medium) or 1400(high) m^3air/h/m fabric]. Fiber diameter, alignment, and baseline bidirectional tensile mechanical properties were evaluated. Attachment and spreading of human adipose-derived stem cells (hASCs) were evaluated over 3 days immediately following seeding. After initial screening, the fabric with the greatest Young's modulus and yield stress was selected for 28-day *in vitro* culture and for evaluation of tendon-like extracellular matrix production and development of mechanical properties. As expected, airflow velocity of the polymer during meltblowing demonstrated an inverse relationship with fiber diameter. All fabrics exhibited fiber alignment parallel to the direction of collector rotation. All fabrics demonstrated mechanical anisotropy at baseline. Cells attached, proliferated, and spread on all fabrics over the initial three-day culture period. Consistent with the observed loss of integrity of the unseeded biomaterial, hASC-seeded scaffolds demonstrated a significant decrease in Young's modulus over 28 days of culture. However, dsDNA, sulfated glycosaminoglycan, and collagen content increased significantly over 28 days. Histology and polarized light microscopy demonstrated collagen deposition and alignment throughout the thickness of the scaffolds. While fiber diameters approximated an order of magnitude greater than those previously reported for electrospun scaffolds intended for tendon tissue engineering, they were still within the range of collagen fiber diameters found in healthy tendon. The extent of matrix production and alignment was similar to that previously observed for multilayered electrospun scaffolds. While the Young's modulus of scaffolds after 28 days of culture was lower than native rotator cuff tendon, it approximated that reported previously following culture of electrospun scaffolds and was on the same order of magnitude as of current Food and Drug Administration-approved patches for rotator cuff augmentation. Together, these data suggest that with minor polymer and parameter modifications, meltblown scaffolds could provide an economical, high-throughput production alternative method to electrospinning for use in rotator cuff tendon tissue engineering.

Keywords: collagen, tendon, meltspun, meltblown, electrospun, rotator cuff

Introduction

Each year, over 4.8 million people visit hospitals for shoulder pain, and over 300,000 surgeries are performed for rotator cuff repair in the United States.[1] Unfortunately, rotator cuff repair has an overall retear rate of around 20% and can be as high as a 94% for large tears.[2,3] Tissue engineering could represent a way forward and improve rotator cuff tendon form and function after injury through combining scaffolds, biomimetic factors, and cells to stimulate regeneration rather than repair of native tissue. Fiber-based scaffolds produced by electrospinning have been evaluated widely for tendon tissue engineering.[4–9] Electrospinning is easy to set up in the laboratory for *in vitro* and preclinical studies, forms nano- or microfibers on a similar size scale as the collagen fibers found in tendon matrix, and can produce

[1]Department of Basic Medical Science, Purdue University College of Veterinary Medicine and Department of Biomedical Engineering, Weldon School of Engineering, Purdue University, West Lafayette, Indiana.
[2]Department of Orthopaedic Surgery, Duke University, Durham, North Carolina.
[3]The Nonwovens Institute, North Carolina State University, Raleigh, North Carolina.
Presented, in part, at the Orthopedic Research Society Annual Meeting, San Diego, 2017.

*This article is part of a special focus issue on Strategic Directions in Musculoskeletal Tissue Engineering. Additional articles can be found in Tissue Engineering Part A, volume 23, numbers 15–16 and Tissue Engineering Part B, number 4.

highly aligned fibers, which is a critical microarchitectural cue for aligned tendon neomatrix synthesis.[10,11] However, electrospun scaffolds have major limitations with respect to production on a commercially relevant scale, for example, multilayered scaffolds of dimensions $1 \times 50 \times 75$ mm take 2–4 h each to fabricate in our laboratory (data not shown), and Tzezana *et al.* calculated electrospun scaffolds accumulate at a rate of 0.8–82.3 mm^3/min.[12]

The meltblowing process was first patented in 1939 as a method for producing nonwoven fabrics from polymers.[13] In meltblowing, the polymer is melted and is then extruded through die heads. Upon exiting the die, the air streams draw out the polymer melt stream into fine fibers where they cool and solidify in ambient air. A thin layer of fibers, therefore, accumulates onto the collection surface, forming a nonwoven fabric.[14,15] The meltblowing process is easy to industrialize and is highly tunable: both the die heads and the surfaces onto which the polymer is extruded can be manipulated, while still forming micro- and nanofibers. In stark contrast to electrospinning, the meltblowing apparatus can create fabrics at a rate up to 5000 m/min.[16] Fiber diameter, density, and alignment can be changed by altering the size of the die capillaries, the number of dies, and the velocity of airflow.

There have been limited previous studies to evaluate meltblown fabrics for tissue engineering purposes, but promising work has assessed this technique for vascular tissue engineering.[17] Additional recent studies confirmed that meltblown and other nonwoven poly(lactic acid) (PLA) fabrics supported attachment,[18] proliferation, and differentiation of human adipose-derived stem cells (hASCs) toward osteogenic and adipogenic lineages[14,19] to a similar extent as single-layer electrospun PLA scaffolds. To the best of our knowledge, meltblown scaffolds have not been evaluated for tendon tissue engineering. Furthermore, these previous studies used induction media to induce lineage specific differentiation.[14,17,19] In contrast, we have not previously used tissue-specific induction media or exogenous growth factors in our rotator cuff tendon tissue engineering studies,[4,11] since this approach could confer several regulatory advantages and could be beneficial if the expression of multiple tissue lineages is desired within the same scaffold. In the current study, our *overall* aim was to evaluate meltblown fabrics for use in rotator cuff tendon tissue engineering. Therefore, our specific aims were to (1) characterize meltblown fabric produced using three PLA blends and several different fabrication parameters, (2) to investigate attachment and proliferation of hASCs on these meltblown nonwoven scaffolds, and (3) to determine if these scaffolds could be used to induce a tendon-like phenotype from hASCs cultured without exogenous growth factors. Our hypothesis was that hASCs would attach to the scaffolds and produce a tendon-like extracellular matrix to a similar extent as our previous findings using multilayered electrospun scaffolds, but that there would be no effect of polymer crystallinity or airflow velocity.

Materials and Methods

Meltblown scaffolds

Bolts of meltblown PLA fabrics were produced at the Nonwovens Institute on the Centennial Campus of North Carolina State University (Raleigh, NC) using one of three different crystallinities of PLA (6100D, 6202D, and a 50:50 blend of 6100/6202D (NatureWorks, Minnetonka, MN). The 6100D crystallinity was nominally 99.5% L-PLA and 0.4% D-PLA, with a relative viscosity of 3.1, while the 6202D crystallinity was nominally 98% L-PLA and 2% D-PLA, with a relative viscosity of 3.1. Each test fabric was produced using several airflow velocities, 1400 (high: Roll A), 900 (medium: Roll B and C), or 500 (low: Roll D) cubic meters of air per hour per meter of fabric. The dimensions of each provided fabric sample from each available roll were 1.5×2.5 m. The 2.5 m aspect was designated the long axis of the fabric and was parallel to the direction of airflow during fabrication (perpendicular to the orientation of the collector).

Fiber diameter and scaffold alignment analysis

Three 3×10 mm strips were cut from the center of each sheet of fabric, and from the edge at the midpoint of the long axis, with the long axis of the strip cut parallel to the long axis of the fabric. The strips were sputter coated with gold, and each sample was viewed using a 501 Philips scanning electron microscope as described previously.[4] Three images were taken per sample, and the diameter of ~ 50 randomly selected fibers per image was measured in ImageJ (NIH). Alignment of fibers within each fabric sample was evaluated by fast Fourier transform using a custom MATLAB (Mathworks, Natick, MA) code as described previously.[20]

Mechanical testing—initial screening

Scaffolds were tested in two separate experiments: An initial screening of tensile mechanical properties of each roll and blend to establish the airflow velocity during fabrication (Roll), most likely to be useful in rotator cuff tendon tissue engineering, followed by a separate experiment in which the three polymer blends produced using identical parameters were either left unseeded or seeded with hASCs then maintained in cell culture for 0 and 28 days to assess the effect of PLA crystallinity and cell-seeding on tensile mechanical properties. For all mechanical testing experiments, scaffolds were cut in dog-bone shapes oriented parallel and perpendicular to the long axis of the fabric ($n = 6$ per group). Verhoeff stain lines were placed at the center and 5 mm on either side of center to allow optical strain analysis.[4] Initial scaffold thickness was measured using a Prosilica GX 1050 digital camera (Allied Vision Technologies, Inc.) and digital calipers in ImageJ. Prewetted or precultured scaffolds were sandwiched in 80-grit sandpaper, mounted, and clamped in the load frame and tested with a 0.5 g preload at a 1% s^{-1} strain rate to failure using an electromechanical testing system (Bose Enduratec Smart Test Series; Bose Corporation) with a 2.27 kg load cell (Sensotec Model 31; Honeywell International). Midsubstance stretch was calculated from digital images acquired at 20 Hz and interpolated to load frame data using custom MATLAB code[4] and Microsoft Excel (Microsoft Office) to calculate Young's modulus, yield stretch, and stress as described previously.

Cell seeding

10×30 mm samples were cut from each scaffold with the long axis parallel to the long axis of the fabric. Scaffolds were disinfected in successively decreasing concentrations of ethanol in phosphate-buffered saline (PBS) for 30 min each. Then

each side of the scaffold was sterilized under ultraviolet radiation for 10 min and prewetted with 25 μL of media. hASCs (Passage 4) previously isolated from the same anatomic depot by collagenase digestion of lipoaspirate surgical waste from three deidentified female donors (age 36–59, body mass index 19.6–33.1), with the approval of the Duke University Institutional Review Board as described,[21] were used as a superlot of cells, prepared at the time of seeding onto scaffolds. For cell attachment, spreading, and initial proliferation studies, scaffolds were seeded by pipetting at a low seeding density of 3×10^5 hASCs/cm^2 to allow single-cell analysis on each side of the scaffold with a 15-min incubation period between seeding of each side. Scaffolds were placed between sterilized Teflon rings in six-well plates coated with 2% agarose, to maintain submersion in culture media, and maintained at 37°C, and 5% CO_2 in Advanced DMEM (Life Technologies) supplemented with 10% fetal bovine serum (Zen-Bio), 1% penicillin–streptomycin–fungizone (Life Technologies), 4 mM L-glutamine (Life Technologies), and 1.5 mM l-ascorbic acid-2-phosphate (Sigma-Aldrich A8960; MW = 289.54) without the use of exogenous growth factors for 0–3 days.[21]

Evaluation of cell attachment, spreading and initial proliferation

Following 4 h of incubation on day 0 and on days 1 and 3 after seeding, scaffolds ($n=2$ per group) were harvested and fixed in 4% paraformaldehyde. The scaffolds were then cut into 8 mm discs before being permeabilized with 0.5% Triton-X. Following incubation with 1:100 Acti-stain 488 (Cytoskeleton, Inc.) and 1:10,000 Hoechst 33342 (Life Technologies) in PBS at room temperature, the scaffolds were mounted on coverslips with glycerol and imaged using a Zeiss Axiovert S100 microscope (Carl-Zeiss). Three images were taken of each sample, then images were imported into Fiji (NIH), and then cell count and cell surface area were calculated using the Bio-Formats plugin. The mean cell density and mean surface area per cell were calculated as measures of cell attachment, proliferation over time, and cell spreading, respectively.

Longer term (28-day) cell culture

Based on initial mechanical testing, cell attachment and spreading data (see Results section), Roll A produced at ''high'' (1400 cubic meters of air per hour per meter of fabric) airflow velocity was selected as the most promising candidate for longer term cell seeding studies. Thus, additional 5×30 mm strips from Roll A for all three polymer blends and additional scaffolds prepared for mechanical testing, as described in Mechanical Testing—Initial Screening section, were seeded with 5×10^5 hASCs/cm^2 on each side in accordance with our previous electrospun studies.[4,11] Unseeded and seeded scaffolds were again placed between sterilized Teflon rings in six-well plates coated with 2% agarose, then maintained in culture as described in Cell Seeding section for 0 or 28 days until harvest. Following harvest, scaffolds were stored at −20°C until analysis.

Mechanical testing—after culture

Before and after 28 days in culture, both unseeded and hASC-seeded Roll A scaffolds underwent tensile testing, as described in Mechanical Testing—Initial Screening section.

Biochemical assays

On days 0 and 28, unseeded and hASC-seeded scaffolds from Roll A for each of the three PLA crystallinities were harvested and lyophilized to obtain dry weight. Scaffolds were minced and digested in papain (125 μg/mL) at 60°C for 1 week. As described previously,[21] the PicoGreen assay (Life Technologies) was used to quantify dsDNA content. Sulfated glycosaminoglycan (s-GAG) content was quantified using 1,9-dimethylmethylene blue dye (pH 3.0) assay.[21,22] Total collagen content was determined by the hydroxyproline assay using a conversion factor of 1:7.46 to convert hydroxyproline to collagen.[21,23] All results were normalized to dry weight (mean ± standard deviation [SD]).

Histology

On day 28, hASC-seeded scaffolds ($n=5$) were harvested and embedded in optimal cutting temperature gel (Sakura) and frozen at −80°C. Following cryosectioning, 10 μm sections were mounted on slides. Slides were stained with either picrosirius red or safranin-O/fast green to evaluate for collagen and s-GAG synthesis. Slides stained with picrosirius red were additionally evaluated with polarized light microscopy at 5-° increments of the polarizer angle to evaluate for alignment of fibrillar collagen.[10,11] To detect collagen alignment for a given fabric, differences between mean pixel intensity and polarizer angle were tested using repeated measures analysis of variance (ANOVA), as described previously.[10]

Statistical analyses

Data are reported as mean ± SD or median (25th quartile, 75th quartile). Parametric data meeting the assumptions for factorial ANOVA were evaluated for the effect of polymer crystallinity, roll, seeding, and time. The Tukey *post hoc* test was used to determine differences between treatments following ANOVA. The fiber diameters were not normally distributed; therefore, the Kruskal–Wallis test was used to compare the ranks across multiple comparisons of this data set, and the Mann–Whitney-U test was used to compare the medians using pairwise comparison. In this case, we found no difference in results ($p<0.05$) between using the Kruskal–Wallis test and the Mann–Whitney-U test. For clarity of presentation, the results of the Mann–Whitney-U comparison were reported for data reported as median (25th, 75th quartiles) in Figure 1C, while the data distributions for all groups evaluated and results of the Kruskal–Wallis test are displayed in Supplementary Figure S1 (Supplementary Data are available online at www.liebertpub.com/tea). Significance was reported at the 95% confidence level for all analyses ($\alpha=0.05$). All statistical comparisons were made using SAS University Edition (SAS Institute, Cary, North Carolina).

Results

Fiber diameter, thickness, and scaffold alignment

Representative gross and SEM images of all four rolls prepared from 6100D crystallinity PLA are shown (Fig. 1a, b). Fiber packing was subjectively greater for Rolls A and B, although this was not quantified. There was no significant effect of PLA crystallinity on fiber diameter within each airflow velocity (i.e., roll) (Fig. 1c, and Supplementary Fig. S1), and

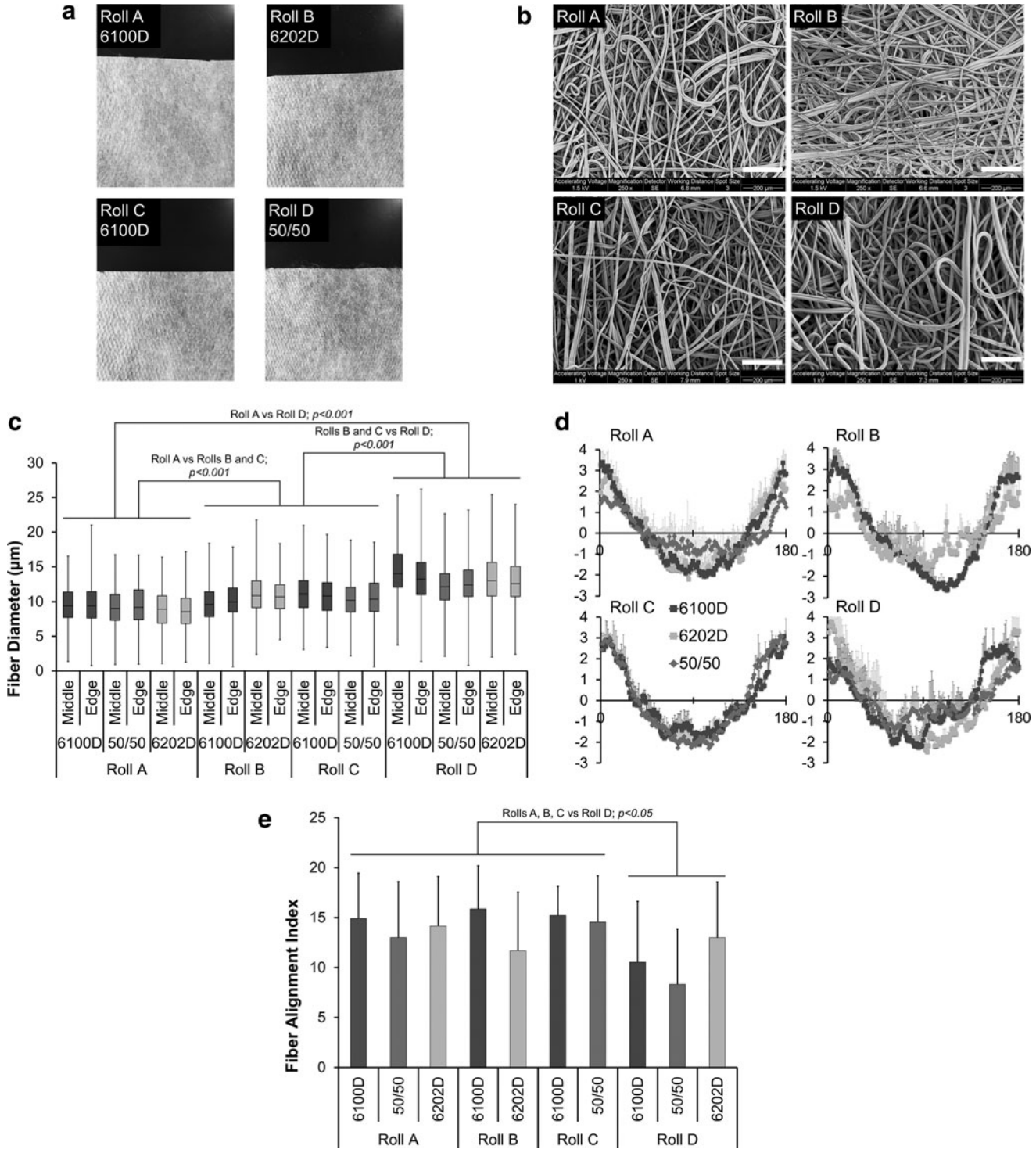

FIG. 1. Representative images **(a)** and scanning electron micrographs **(b)** from four different rolls of 6100D crystallinity poly(lactic acid) (PLA) meltblown fabric. Scale bar in **(b)** represents 200 µm. **(c)** Fiber diameters represented by box and *whiskers plot*:*line* reporting median fiber diameter, box reporting first and third quartile; *whiskers* signifying minimum and maximum values from the edge and middle of each sheet of meltblown fabric ($n = 3$, 3 images/scaffold, 50 fibers/image). *p*-values marked above bars represent difference between rolls (Mann–Whitney-U Test; *p*-values the same for both Kruskal–Wallis and Mann–Whitney-U; see Supplementary Figure S1 for full data distributions) **(d)** fast Fourier transform of scaffolds cut from each roll for all PLA crystallinities ($n = 6$, 3 images/scaffold; mean ± SD), with peaks in amplitude at 0 and 180° corresponding to long axis of fabric and direction of collector rotation. **(e)** Fiber alignment index for each meltblown fabric (mean ± SD). *p*-values marked above bars represent differences between rolls (ANOVA). ANOVA, analysis of variance; SD, standard deviation.

location of fiber within the fabric (middle vs. edge) also did not influence fiber diameter, but the effect of airflow velocity was significant, since fiber diameters of Roll A fabrics (median 8.7–9.4 μm) were significantly less than for Rolls B (median 9.8–10.8 μm) and C (median 10.3–10.9 μm), with Roll D fabrics having the greatest fiber diameters (median 12.2–13.6 μm). The thickness of nonwoven fabric scaffolds ranged from 0.25 ± 0.03 mm to 0.30 ± 0.05 mm. There was a trend toward increased thickness of Roll D scaffolds ($p = 0.0535$) compared with other rolls but there was no effect of polymer crystallinity on thickness (Supplementary Table S1). All rolls and crystallinities demonstrated some degree of fiber alignment (Fig. 1d) parallel to the long axis of the fabric (assigned to 0 and 180 degrees), that is, parallel to the direction of airflow and the travel of the collector. There was no significant effect of crystallinity on fiber alignment index (Fig. 1e), but rolls A–C, produced with greater airflow velocities demonstrated significantly greater fiber alignment indices than Roll D.

Mechanical testing—initial screening

At baseline, all scaffolds showed anisotropy with respect to Young's modulus and yield stress in a direction parallel to the long axis of the fabric (Fig. 2 for 6100D blend and Supplementary Fig. S2 for other blends). Scaffolds prepared from Roll A had significantly greater Young's modulus (Fig. 2c) and yield stress (Fig. 2d) ($p < 0.0001$) than scaffolds prepared from other rolls. Yield stretch did not demonstrate significant anisotropy, except for Roll B. PLA polymer crystallinity had no significant effect on the tensile mechanical properties evaluated.

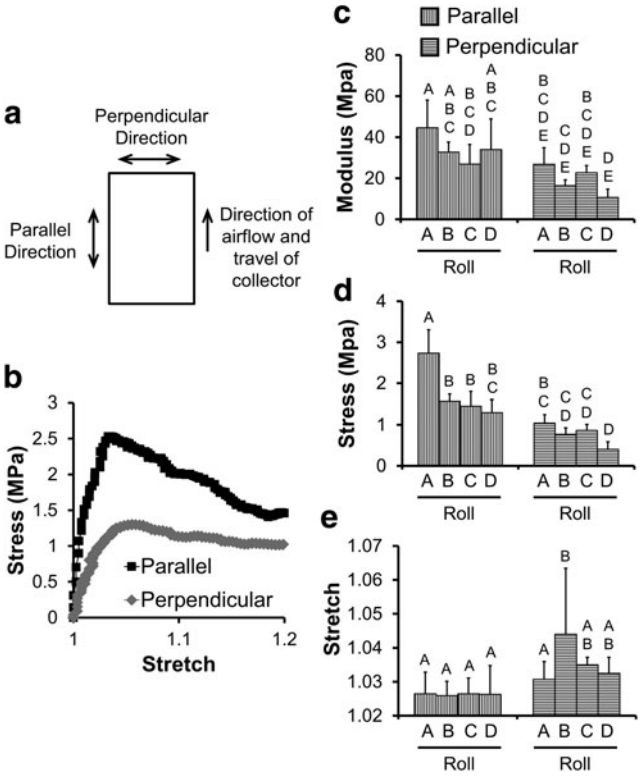

FIG. 2. **(a)** Schematic of the meltblown fabric sheet demonstrates the direction of mechanical testing in relation to the direction of travel of the collector for the meltblowing apparatus. Representative stretch-strain curve **(b)** for 6100D PLA meltblown scaffolds taken from Roll A. Mean ± SD Young's modulus **(c)** yield stress **(d)**, and yield stretch **(e)** in 6100D PLA meltblown scaffolds tested in orthogonal directions, $n = 6$. Groups with *different letters* above are significantly different from each other, $p < 0.05$. Data for other blends of PLA can be found in Supplementary Figure S2.

Cell attachment and spreading

hASCs attached to all scaffolds with no significant effect of PLA crystallinity or roll and cell density was significantly greater on days 1 and 3 ($p = 0.0007$) compared with day 0 (Fig. 3a and Supplementary Fig. S3a). Cell surface area (Fig. 3b and Supplementary Fig. S3b) increased by day 3 compared with day 0 ($p < 0.0001$) and cells seeded on roll D spread to a greater extent than cells seeded on the other rolls ($p = 0.0008$).

Mechanical testing—after culture

Following 28 days of culture, unseeded, Roll A scaffolds tore easily, and the majority of unseeded scaffolds failed before tensile testing could be accomplished. In contrast, for hASC-seeded scaffolds after 28 days in culture, while the Young's modulus (Fig. 4) decreased significantly compared with day 0 ($p < 0.0001$), there was no effect of time in culture for yield stress or yield stretch. The 6100D PLA had a significantly greater yield stress at both days 0 and 28 than the other PLA crystallinities ($p = 0.0093$).

Biochemical assays

Scaffold dry weight did not significantly change between unseeded scaffolds harvested on day 0 and those cultured for 28 days (data not shown). dsDNA, s-GAG, and collagen

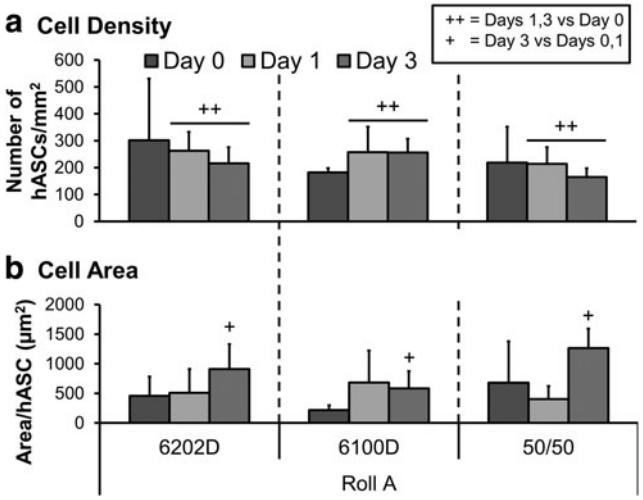

FIG. 3. Mean ± SD cell density **(a)** and single cell area **(b)** ($n > 10$ cells/image; six images per scaffold) of human adipose stem cells cultured for 0 (harvested at 4 h), 1, and 3 days on meltblown scaffolds of various PLA crystallinities [6100D, 6202D and a 50/50 blend] from Roll A fabrics ($n = 2$, measurements from three images [0.3 mm^2] per scaffold). For complete data set refer to Supplementary Figure S3. $^{++}$Difference between days 1 and 3 and day 0. $^{+}$Difference between day 3 and days 0 and 1.

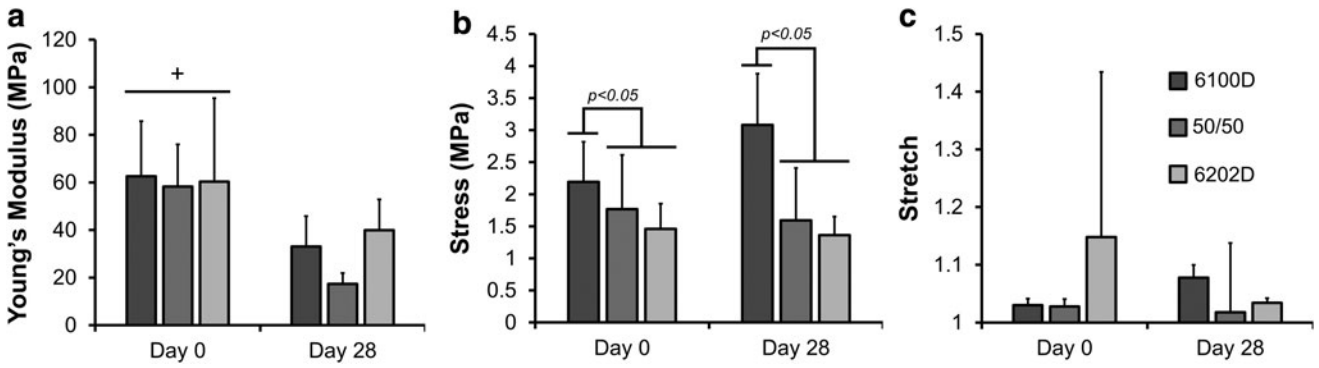

FIG. 4. Mean ± SD Young's modulus **(a)**, yield stress **(b)**, and yield stretch **(c)** in hASC-seeded Roll A PLA scaffolds after 0 and 28 days of culture, (n = 3-6). $^{+}$Significant difference between day 0 and 28; p-values marked above bars represent significant difference between the 6100D PLA and the 50/50 and 6200D PLA crystallinities ($p \leq 0.05$, ANOVA; Tukey's *post-hoc* test). hASC, human adipose-derived stem cell.

content (Fig. 5) increased in all Roll A scaffolds after 28 days of culture for the seeded scaffolds ($p < 0.0001$). No significant effect of polymer was identified except that scaffolds containing 6100D were found to have a significantly increased s-GAG concentration compared with the pure 6202D scaffolds ($p = 0.0180$). There was a trend ($p = 0.0534$) for the 6100D scaffolds to also have a greater collagen content than blends containing 6202D.

Histology

Histology (Fig. 6) demonstrated collagen deposition and as expected, no s-GAG detectable by safranin-O staining throughout the full thickness of all Roll A scaffolds. There were small areas of the scaffold that were incompletely filled by extracellular matrix, representing either PLA fibers or incomplete matrix formation. Polarized light microscopy of picrosirius red-stained images confirmed substantial aligned fibrillar collagen (Fig. 6c) formation, which when quantified at 5° increments of the polarizer angle demonstrated peak mean pixel intensity in direction of the long axis of the fabric (Fig. 6d); there was no significant effect of PLA blend on degree of aligned collagen fibril formation.

Discussion

High-throughput meltblown fabrics produced using several airflow velocities and PLA crystallinities had fiber diameters in the 8–14 μm range and demonstrated a mean baseline anisotropy of 1.94 ± 0.58. All fabrics supported cell attachment, proliferation, and spreading over an initial 3-day period. Over 28 days of culture, scaffolds prepared from Roll A (highest airflow velocity) supported continued cell proliferation and aligned tendon-like matrix formation throughout the full thickness of the scaffold. Despite rapid degradation of the underlying PLA scaffold over 28 days in culture in unseeded scaffolds, the yield stress of hASC-seeded Roll A scaffolds was maintained through the culture period.

We and others have evaluated electrospinning extensively for use in tendon tissue engineering.[4–9,11] A major attraction of this technique is the ability to form scaffolds from nanofibers on the scale of 3–5000 nm,[24] which allows for the production of fibers on a similar scale to the collagen fibrils found in healthy tendon matrix *in vivo*.[5,25–27] These fiber diameters are biomimetic and provide relevant physiological

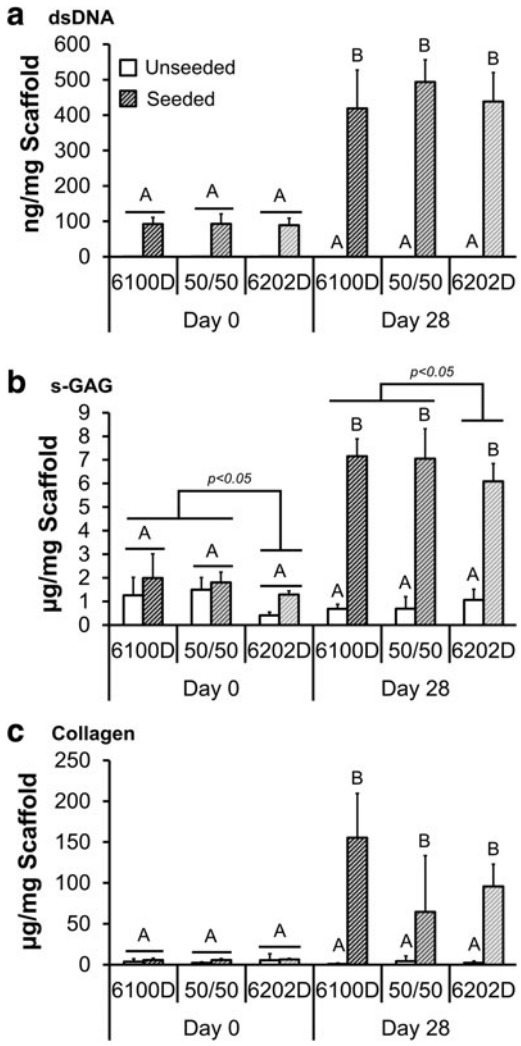

FIG. 5. Mean ± SD dsDNA **(a)**, sulfated glycosaminoglycan (s-GAG) **(b)**, and collagen **(c)** content of scaffolds prepared using various crystallinities of PLA but with consistent fabrication parameters (Roll A) 0 and 28 days after seeding with 5×10^5 hASC/cm^2. (n = 5) Groups with *different letters* above are significantly different from each other; p-values marked above bars represent significant difference between PLA crystallinities, ($p \leq 0.05$, ANOVA; Tukey's *post hoc* test).

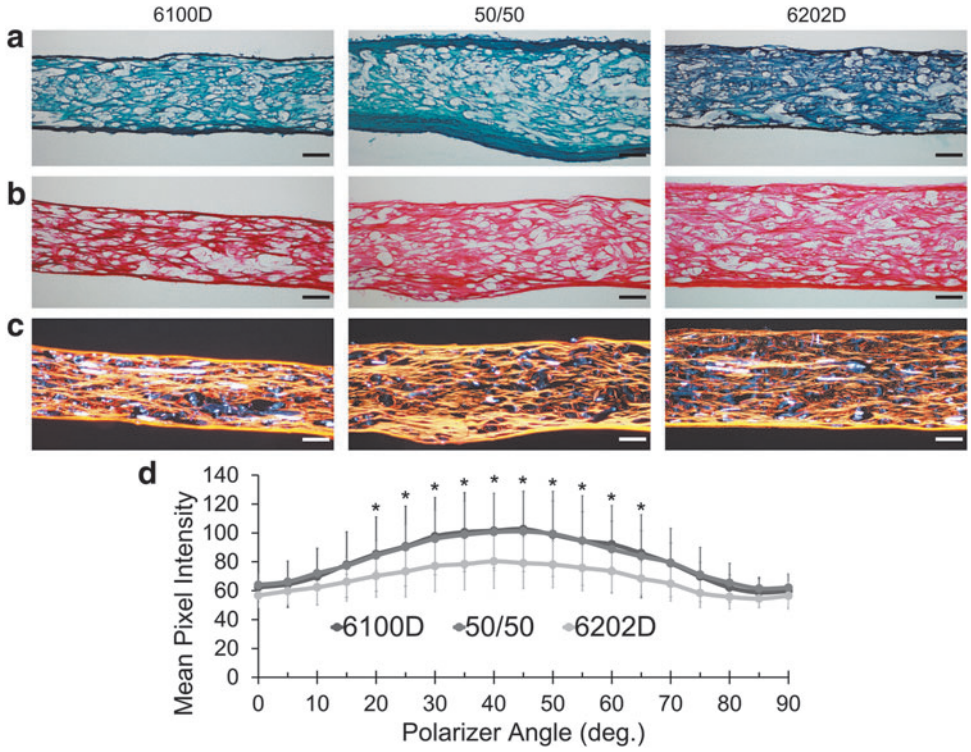

FIG. 6. Safranin-O/fast green staining under visible light **(a)**, picrosirius red staining under visible **(b)** and *orange/red* birefringence observed under polarized light **(c)** for scaffolds from Roll A of three different PLA crystallinities cultured for 28 days with hASCs. Scale bar represents 100 μm. Mean ± SD pixel intensity of *orange/red* birefringence at each assessed polarizer angle, with 45° **(d)** ($n = 3$) corresponding to the direction of the collector of the meltblowing apparatus. *Difference between mean pixel intensity and intensity at 0° polarizer angle for all blends, ($p < 0.05$, repeated measures ANOVA, Tukey *post hoc* test). Color images available online at www.liebertpub.com/tea

structure for tendon-like extracellular matrix synthesis by both differentiated tendon fibroblasts and various stem cell lineages, particularly as the alignment of the fibers increases.[10,11,28,29] For example, electrospun fibers with mean diameters between 380 and 1800 nm were investigated for their ability to modulate cell alignment, gene expression, and tendon-like matrix synthesis.[5,29] The larger fiber diameters promoted cell alignment and a phenotype more consistent with tendon, but the upper threshold of a beneficial effect of large fiber diameter was not established. In contrast, previous studies using a variety of cell types seeded on grooves and channels from 0.5 to 25 μm wide generated by photolithography have shown that smaller channel width and smaller repeat spacing of grooves generally increase elongation and orientation of cells compared with wide channels or widely spaced channels.[30] Therefore, extrapolation of cell adhesion, proliferation, migration, and differentiation behavior from photolithography to fiber-based scaffolds could be difficult.

All fabrics exhibited limited fiber alignment and mechanical anisotropy in direct proportion to airflow velocity, despite no concerted attempt to produce aligned fibers in this study. Roll D fabrics demonstrated significantly less fiber alignment than fabrics from other rolls, likely because of the lower airflow velocity during fabrication. Despite a significantly greater yield stress and Young's modulus compared with other rolls of fabric, Roll A did not exhibit significantly increased alignment compared with all other rolls, and Roll A had a significantly lower fiber diameter than all other rolls, but the fiber packing density was subjectively greater in Rolls A and B than Rolls C and D. Based on these data, it is possible that fiber density, packing, and cell–fiber interactions played a role in the enhanced mechanical properties, however, this was not evaluated in the current study. However, given the importance of initial mechanical properties for a rotator cuff augmentation device, this was the primary reason why Roll A was selected for evaluation over the 28-day culture period.

Recent data comparing electrospun PLA scaffolds with meltblown PLA scaffolds suggest that hASC adhesion and proliferation are not attenuated by increasing fiber diameter.[14] In this study, hASCs seeded on Roll D scaffolds exhibited a larger surface area than cells seeded on other rolls. The reasons for this are not known, but studies are going on to evaluate cell–fiber diameter and cell–fiber packing interactions. In the current study, biochemical content, histology, and mechanical testing results were in many respects comparable to our previous rotator cuff tendon tissue engineering work using multilayered electrospun scaffolds produced using similar cell donors and identical culture conditions,[4,11] suggesting that the fiber diameters up to at least 15 μm do not impede deposition of a tendon-like matrix. Higher s-GAG concentrations were observed on Roll A scaffolds containing 6100D PLA, and there was a trend ($p = 0.0534$) for 6100D scaffolds to have greater collagen concentrations, possibly contributing to the increased yield stress observed in seeded 6100D scaffolds. Consistent with our previous work,[31] we would not expect positive safranin-O staining until the s-GAG concentration exceeds 1% dry weight (10 μg/mg). A major difference observed using these scaffolds compared with our previous work with electrospun scaffolds was that collagen content normalized by weight following 28 days of culture in these scaffolds was almost 10-fold higher than that observed previously.

This increase in collagen content was in agreement with the results of Erisken *et al.* that larger fiber diameters lead to an increase in type I collagen and tenomodulin expression by human rotator cuff fibroblasts,[5] and suggests that improved understanding of the upper limit of biomimetic fiber diameters would be beneficial to tendon tissue engineering and to enhanced understanding of the interactions of focal

adhesion complexes and early fibronectin matrix assembly with biomaterials and subsequent collagen fibrillogenesis.[32,33] In contrast to our current results and to the results of others,[5] Bashur *et al.*, found that a *smaller* fiber diameter (280 nm vs. 820 nm and 2300 nm) resulted in increased type I collagen production along with increased decorin and tenomodulin expression in a rat bone marrow-derived mesenchymal stem cell model.[34] Thus, it is apparent from these studies that there could be a differential effect of fiber diameter depending on cell type or species. In human mesenchymal stem cells, fibers with a diameter of 15 μm induced adipogenesis,[35] fibers 2 μm in diameter induced osteogenesis,[35] while fibers ~300 nm in diameter induced chondrogenesis,[36] all without tissue-specific induction media. Our results from this study suggest that fibers in the 9 μm range result in a tendon-like phenotype when cultured with hASCs in the absence of specific growth factors. By any measure, more work is needed to understand the effect that fiber diameter plays on tenogenic differentiation.

To the best of our knowledge, neither fiber alignment nor mechanical anisotropy has been reported previously for meltblown fabrics. Surprisingly, all meltblown fabrics provided showed alignment parallel to the direction of travel of the collector, and airflow velocity was related to the degree of alignment. Previous electrospinning studies show that alignment of electrospun fibers is beneficial for mechanical properties,[11,29,37] promotes expression of tenogenic markers,[38] and governs matrix alignment.[29,38] Substantial, aligned type I collagen developed on the scaffolds over a 28-day culture period suggests that cellular elongation and alignment were also present,[10] although these factors were not evaluated in this study. While the degree of mechanical anisotropy in these meltblown fabrics was substantially less than that reported for electrospun scaffolds and for supraspinatus tendon of the rotator cuff,[11,39,40] the production parameters of the meltblown assembly could be manipulated to permit introduction of increased mechanical anisotropy. Overall, the modulus of scaffolds in this study was still around 30% of native supraspinatus tendon,[39] but was on the same order of magnitude as Food and Drug Administration-approved extracellular matrix (ECM) and synthetic scaffolds.[41,42] The meltblown fabrics used in this study are thin enough to allow for intra-operative deployment through an arthroscopic portal. This represents an additional advantage for translation should further study and refinement of these fabrics continue to be as encouraging as this initial *in vitro* study.

Although matrix synthesis and aligned collagen were observed throughout the thickness of the scaffold, there were focal areas where no matrix was present, something that we have not previously observed with electrospun scaffolds.[4,11] These regions were too large in cross section to represent the fibers within the scaffolds, and have not been identified as a cryosectioning artifact previously. The cause of the incomplete matrix ''fill'' is unknown and is the subject of ongoing investigation, but could represent interactions between biomaterial factors (such as fiber diameter, alignment, and packing [inter-fiber distance]) and the number of fiber interactions of each individual cell, which could potentially limit interfiber matrix synthesis.

The rapid degradation of unseeded PLA scaffolds over 28 days of *in vitro* culture was surprising since PLA is known for its relatively long degradation time,[43–45] however, similar rapid degradation has been observed by Pavia *et al.* for PLA foams under standard culture media conditions. In this case, approximately 20% loss of dry weight was observed after 30 days culture in DMEM/FBS.[46] However, we observed no significant loss of dry weight in the unseeded PLA meltblown scaffolds after 28 days in culture, but initial and day 28 dry weights were not obtained by repeated measures of the same scaffolds. The 6100D and 6202D blends of PLA used in these studies were specifically intended for fiber processes but were marketed for food packaging rather than biomedical applications. Despite this, the glass transition temperatures and crystalline melt temperatures of these blends were similar to those reported for medical grade PLA. Processing of PLA to protect the thermal stability of the polymer is critical to prevent thermal degradation, the effect of which is to reduce molecular weight and to potentially render the polymer more susceptible to accelerated biodegradation.[44] In future studies, additional optimization of the meltblowing process factors, such as moisture level, residence time, and temperature, could help preserve the thermal stability of the polymer and subsequently the *in vitro* and *in vivo* degradation rate. Evaluation of molecular weight of the PLA or accumulation of degradation products in culture media could offer further perspectives in future studies, should other limitations of PLA for rotator cuff tendon tissue engineering and tendon-bone regeneration be addressed. Future studies will also examine the question of whether an alternative polymer could further enhance meltblown fabrics for rotator cuff tendon tissue engineering.

We did not examine the porosity or fiber density of the fabrics. The density of fibers and size of the pores could have played a role in cell–fiber interactions, matrix synthesis, and in the tensile mechanical properties; future studies to refine the application of meltblown scaffolds will evaluate these parameters. We also did not investigate tendon-related gene expression on these scaffolds, given the poor correlation between differential tendon-related gene expression and development of a tendon phenotype on fiber-based scaffolds,[4,5,10,11,29] but are currently working, as are others, to identify definitive markers of tendon, tendon cell identity, and engineered tendon development. Nonetheless, the observed robust aligned collagen synthesis, negative staining for safranin-O by histological evaluation, and high collagen:s-GAG ratio, as assessed by biochemical analysis are more consistent with deposition of a tendon-like extracellular matrix than with other expected tissue phenotypes. However, we did not specifically eliminate the possibility of adipogenic, chondrogenic, or osteogenic differentiation in the current study. Notwithstanding the relatively large fiber diameters in the current study compared with our previous studies using single- and multilayered electrospinning, gene expression profiles associated with these ''off-target'' phenotypes in hASCs have not been observed on electrospun scaffolds without the use of specific induction media or of incorporation of tissue-specific biomimetic factors into the scaffolds,[31] but these molecular markers will be evaluated in future studies.

Conclusion

Together, these results confirm that meltblown fabrics are biomimetic for hASCs and permit cell attachment, spreading, proliferation, and demonstrate synthesis of an

aligned tendon-like extracellular matrix. Meltblown fabrics produced at highest airflow velocities increased fiber alignment and anisotropy and had increased yield stress and Young's modulus compared with fabrics produced using lower airflow velocities; these outcomes are essential for tendon tissue engineering. With respect to PLA and crystallinity, pure 6100D may be more suitable than 6202D or blends, given the increase in yield stress and trend toward inducing increased collagen synthesis observed, but these findings await further validation. The meltblowing process is a high-throughput process, which may offer several advantages over electrospinning for the purposes of commercialization. Further manipulation of fabrication parameters could further optimize opportunities for this technology in tendon tissue engineering.

Acknowledgments

Research reported in this publication was supported by the National Institute of Arthritis and Musculoskeletal and Skin Diseases of the National Institutes of Health under Award Nos. AR065764 (DL) and AR059784 (DL). The content is solely the responsibility of the authors and does not necessarily represent the official views of the National Institutes of Health.

Disclosure Statement

No competing financial interests exist.

References

1. Colvin, A.C., Egorova, N., Harrison, A.K., Moskowitz, A., and Flatow, E.L. National trends in rotator cuff repair. J Bone Joint Surg Am **94,** 227, 2012.
2. Galatz, L.M., Ball, C.M., Teefey, S.A., Middleton, W.D., and Yamaguchi, K. The outcome and repair integrity of completely arthroscopically repaired large and massive rotator cuff tears. J Bone Joint Surg Am **86-A,** 219, 2004.
3. Wu, X.L., Briggs, L., and Murrell, G.A. Intraoperative determinants of rotator cuff repair integrity: an analysis of 500 consecutive repairs. Am J Sports Med **40,** 2771, 2012.
4. Chainani, A., Hippensteel, K.J., Kishan, A., Garrigues, N.W., Ruch, D.S., Guilak, F., and Little, D. Multilayered electrospun scaffolds for tendon tissue engineering. Tissue Eng Part A **19,** 2594, 2013.
5. Erisken, C., Zhang, X., Moffat, K.L., Levine, W.N., and Lu, H.H. Scaffold fiber diameter regulates human tendon fibroblast growth and differentiation. Tissue Eng Part A **19,** 519, 2013.
6. Huegel, J., Kim, D.H., Cirone, J.M., Pardes, A.M., Morris, T.R., Nuss, C.A., Mauck, R.L., Soslowsky, L.J., and Kuntz, A.F. Autologous tendon-derived cell-seeded nanofibrous scaffolds improve rotator cuff repair in an age-dependent fashion. J Orthop Res **35,** 1250, 2017.
7. Lee, C.H., Shin, H.J., Cho, I.H., Kang, Y.M., Kim, I.A., Park, K.D., and Shin, J.W. Nanofiber alignment and direction of mechanical strain affect the ECM production of human ACL fibroblast. Biomaterials **26,** 1261, 2005.
8. Sahoo, S., Ouyang, H., Goh, J.C., Tay, T.E., and Toh, S.L. Characterization of a novel polymeric scaffold for potential application in tendon/ligament tissue engineering. Tissue Eng **12,** 91, 2006.
9. Sheikh, F.A., Macossay, J., Cantu, T., Zhang, X., Shamshi Hassan, M., Esther Salinas, M., Farhangi, C.S., Ahmad, H., Kim, H., and Bowlin, G.L. Imaging, spectroscopy, mechanical, alignment and biocompatibility studies of electrospun medical grade polyurethane (Carbothane 3575A) nanofibers and composite nanofibers containing multiwalled carbon nanotubes. J Mech Behav Biomed Mater **41,** 189, 2015.
10. Gilchrist, C.L., Ruch, D.S., Little, D., and Guilak, F. Micro-scale and meso-scale architectural cues cooperate and compete to direct aligned tissue formation. Biomaterials **35,** 10015, 2014.
11. Orr, S.B., Chainani, A., Hippensteel, K.J., Kishan, A., Gilchrist, C., Garrigues, N.W., Ruch, D.S., Guilak, F., and Little, D. Aligned multilayered electrospun scaffolds for rotator cuff tendon tissue engineering. Acta Biomater **24,** 117, 2015.
12. Tzezana, R., Zussman, E., and Levenberg, S. A layered ultraporous scaffold for tissue engineering, created via a hydrospinning method. Tissue Eng Part C Methods **14,** 281, 2008.
13. Rasmus, P.W. Polyamides. US Patent 2,174,527, October 3, 1939.
14. Haslauer, C.M., Avery, M.R., Pourdeyhimi, B., and Loboa, E.G. Translating textiles to tissue engineering: creation and evaluation of microporous, biocompatible, degradable scaffolds using industry relevant manufacturing approaches and human adipose derived stem cells. J Biomed Mater Res B Appl Biomater **103,** 1050, 2015.
15. Little, D., Pourdeyhimi, B., and Jenkins, T. High Throughput Non-woven Fabrics for Soft Tissue Repair and Regeneration. US Provisional Patent 62/358,613, July 6, 2016.
16. Mezghani, K., and Spruiell, J.E. High speed melt spinning of poly(L-lactic acid) filaments. J Polym Sci Part B Pol Phys **36,** 1005, 1998.
17. Moreno, M.J., Ajji, A., Mohebbi-Kalhori, D., Rukhlova, M., Hadjizadeh, A., and Bureau, M.N. Development of a compliant and cytocompatible micro-fibrous polyethylene terephthalate vascular scaffold. J Biomed Mater Res B Appl Biomater **97,** 201, 2011.
18. Hanson, A.D., Wall, M.E., Pourdeyhimi, B., and Loboa, E.G. Effects of oxygen plasma treatment on adipose-derived human mesenchymal stem cell adherence to poly(L-lactic acid) scaffolds. J Biomater Sci Polym Ed **18,** 1387, 2007.
19. Tuin, S.A., Pourdeyhimi, B., and Loboa, E.G. Creating tissues from textiles: scalable nonwoven manufacturing techniques for fabrication of tissue engineering scaffolds. Biomed Mater **11,** 015017, 2016.
20. Garrigues, N.W., Little, D., O'Conor, C.J., and Guilak, F. Use of an insulating mask for controlling anisotropy in multilayer electrospun scaffolds for tissue engineering. J Mater Chem **20,** 8962, 2010.
21. Little, D., Guilak, F., and Ruch, D.S. Ligament-derived matrix stimulates a ligamentous phenotype in human adipose-derived stem cells. Tissue Eng Part A **16,** 2307, 2010.
22. Enobakhare, B.O., Bader, D.L., and Lee, D.A. Quantification of sulfated glycosaminoglycans in chondrocyte/alginate cultures, by use of 1,9-dimethylmethylene blue. Anal Biochem **243,** 189, 1996.
23. Neidert, M.R., Lee, E.S., Oegema, T.R., and Tranquillo, R.T. Enhanced fibrin remodeling in vitro with TGF-beta1, insulin and plasmin for improved tissue-equivalents. Biomaterials **23,** 3717, 2002.
24. Subbiah, T., Bhat, G., Tock, R., Parameswaran, S., and Ramkumar, S. Electrospinning of nanofibers. J Appl Pol Sci **96,** 557, 2005.

25. Fratzl, P. Cellulose and collagen: from fibres to tissues. Curr Opin Colloid Interface Sci **8,** 32, 2003.
26. Kadler, K.E., Holmes, D.F., Trotter, J.A., and Chapman, J.A. Collagen fibril formation. Biochem J **316 (Pt 1),** 1, 1996.
27. Nimni, M., and Harkness, R. Molecular structures and functions of collagen. Collagen **1,** 1, 1988.
28. Kuo, C.K., and Tuan, R.S. Tissue engineering with mesenchymal stem cells. IEEE Eng Med Biol Mag **22,** 51, 2003.
29. Moffat, K.L., Kwei, A.S.P., Spalazzi, J.P., Doty, S.B., Levine, W.N., and Lu, H.H. Novel nanofiber-based scaffold for rotator cuff repair and augmentation. Tissue Eng Part A **15,** 115, 2009.
30. Flemming, R.G., Murphy, C.J., Abrams, G.A., Goodman, S.L., and Nealey, P.F. Effects of synthetic micro- and nano-structured surfaces on cell behavior. Biomaterials **20,** 573, 1999.
31. Garrigues, N.W., Little, D., Sanchez-Adams, J., Ruch, D.S., and Guilak, F. Electrospun cartilage-derived matrix scaffolds for cartilage tissue engineering. J Biomed Mater Res A **102,** 3998, 2014.
32. Hsia, H.C., Nair, M.R., Mintz, R.C., and Corbett, S.A. The fiber diameter of synthetic bioresorbable extracellular matrix influences human fibroblast morphology and fibronectin matrix assembly. Plast Reconstr Surg **127,** 2312, 2011.
33. Kadler, K.E., Hill, A., and Canty-Laird, E.G. Collagen fibrillogenesis: fibronectin, integrins, and minor collagens as organizers and nucleators. Curr Opin Cell Biol **20,** 495, 2008.
34. Bashur, C.A., Shaffer, R.D., Dahlgren, L.A., Guelcher, S.A., and Goldstein, A.S. Effect of fiber diameter and alignment of electrospun polyurethane meshes on mesenchymal progenitor cells. Tissue Eng Part A **15,** 2435, 2009.
35. Abagnale, G., Steger, M., Nguyen, V.H., Hersch, N., Sechi, A., Joussen, S., Denecke, B., Merkel, R., Hoffmann, B., Dreser, A., Schnakenberg, U., Gillner, A., and Wagner, W. Surface topography enhances differentiation of mesenchymal stem cells towards osteogenic and adipogenic lineages. Biomaterials **61,** 316, 2015.
36. Wu, Y., Yang, Z., Law, J.B., He, A.Y., Abbas, A.A., Denslin, V., Kamarul, T., Hui, J.H., and Lee, E.H. The combined effect of substrate stiffness and surface topography on chondrogenic differentiation of mesenchymal stem cells. Tissue Eng Part A **23,** 43, 2017.
37. Mauck, R.L., Baker, B.M., Nerurkar, N.L., Burdick, J.A., Li, W.J., Tuan, R.S., and Elliott, D.M. Engineering on the straight and narrow: the mechanics of nanofibrous assemblies for fiber-reinforced tissue regeneration. Tissue Eng Part B Rev **15,** 171, 2009.
38. Yin, Z., Chen, X., Chen, J.L., Shen, W.L., Hieu Nguyen, T.M., Gao, L., and Ouyang, H.W. The regulation of tendon stem cell differentiation by the alignment of nanofibers. Biomaterials **31,** 2163, 2010.
39. Lake, S.P., Miller, K.S., Elliott, D.M., and Soslowsky, L.J. Tensile properties and fiber alignment of human supraspinatus tendon in the transverse direction demonstrate inhomogeneity, nonlinearity, and regional isotropy. J Biomech **43,** 727, 2010.
40. Lake, S.P., Miller, K.S., Elliott, D.M., and Soslowsky, L.J. Effect of fiber distribution and realignment on the nonlinear and inhomogeneous mechanical properties of human supraspinatus tendon under longitudinal tensile loading. J Orthop Res **27,** 1596, 2009.
41. Derwin, K.A., Baker, A.R., Spragg, R.K., Leigh, D.R., and Iannotti, J.P. Commercial extracellular matrix scaffolds for rotator cuff tendon repair. Biomechanical, biochemical, and cellular properties. J Bone Joint Surg Am **88,** 2665, 2006.
42. Barber, F.A., and Aziz-Jacobo, J. Biomechanical testing of commercially available soft-tissue augmentation materials. Arthroscopy **25,** 1233, 2009.
43. Rezwan, K., Chen, Q.Z., Blaker, J.J., and Boccaccini, A.R. Biodegradable and bioactive porous polymer/inorganic composite scaffolds for bone tissue engineering. Biomaterials **27,** 3413, 2006.
44. Farah, S., Anderson, D.G., and Langer, R. Physical and mechanical properties of PLA, and their functions in widespread applications—a comprehensive review. Adv Drug Deliv Rev **107,** 367–392, 2016.
45. Yang, S., Leong, K.F., Du, Z., and Chua, C.K. The design of scaffolds for use in tissue engineering. Part I. Traditional factors. Tissue Eng **7,** 679, 2001.
46. Pavia, F.C., La Carrubba, V., Piccarolo, S., and Brucato, V. Polymeric scaffolds prepared via thermally induced phase separation: tuning of structure and morphology. J Biomed Mater Res A **86,** 459, 2008.

Address correspondence to:
Dianne Little, DVM, PhD
Department of Basic Medical Sciences
Purdue University
1330 Lynn Hall
625 Harrison Street
West Lafayette, IN 47907

E-mail: little33@purdue.edu

Received: October 26, 2016
Accepted: August 16, 2017
Online Publication Date: September 5, 2017